

# Defects, order, and hysteresis in driven charge-density waves

Mikko Karttunen<sup>1</sup>, Mikko Haataja<sup>1</sup>, K. R. Elder<sup>2</sup>, and Martin Grant<sup>1</sup>

<sup>1</sup>*Department of Physics and Centre for the Physics of Materials, McGill University, 3600 rue University, Montréal (Québec), Canada H3A 2T8*

<sup>2</sup>*Department of Physics, Oakland University, Rochester, MI, 48309-4487*

(April 7, 2018)

We model driven two-dimensional charge-density waves in random media via a modified Swift-Hohenberg equation, which includes both amplitude and phase fluctuations of the condensate. As the driving force is increased, we find that the defect density first increases and then decreases. Furthermore, we find switching phenomena, due to the formation of channels of dislocations. These results are in qualitative accord with recent dynamical x-ray scattering experiments by Ringland *et al.* and transport experiments by Lemay *et al.*

PACS numbers: 71.45.Lr, 72.70.+m, 74.60.Ge

The effect of quenched disorder on a periodic medium has been the subject of intense study during the past decade. The rich phenomena displayed by these systems has raised intriguing questions [1–3]. These include the nature of the depinning transition, the effect of disorder on structural properties, and the possibility of the existence of nonequilibrium analogs of solids and liquids. Examples of such systems include charge-density waves (CDW) [4], flux line lattices in type-II superconductors [5,6], and magnetic bubble arrays [7]. A common effect of quenched disorder in equilibrium systems displaying periodicity is to reduce or destroy that periodicity, by pinning the system in a disordered state. However, a sufficiently large driving force in a nonequilibrium system can act to depin the system, thereby reducing the effect of quenched disorder to that of annealed disorder, analogous to thermal noise.

A CDW is a periodic modulation of the electron density, of wavenumber  $Q$ , which results from the electron-phonon interaction [8]. The local excess density of the conduction electrons is given by  $\rho(\vec{x}, t) = \rho_c(\vec{x}, t) \cos(\vec{Q} \cdot \vec{x} + \phi(\vec{x}, t))$ , where  $Q \equiv 2k_F$ ,  $k_F$  is the Fermi wavenumber,  $\rho_c$  is the CDW amplitude, and  $\phi$  is the phase. It is convenient to introduce a scalar order parameter  $\psi(\vec{x}, t) = \text{Re}[e^{i\vec{Q} \cdot \vec{x}} \rho_c(\vec{x}, t) e^{i\phi(\vec{x}, t)}]$ .

An important question concerns the role of amplitude fluctuations of the condensate close to the depinning transition [9–13]. A common approximation is to neglect amplitude fluctuations, leading to a phase-only description [14–17]. However, this approximation is not always justified, as demonstrated by Coppersmith and Millis [9–11] for a model of a driven CDW, and as argued by Balents and Fisher [12]. Moreover, recent theoretical studies in 2D indicate that dislocations proliferate in the presence of quenched disorder even in the absence of an external driving force [18]. Therefore, the role of amplitude fluctuations close to the depinning transition warrants a closer examination.

To this end, we propose a model for driven CDWs,

and show that dislocations indeed proliferate close to the depinning transition. This behavior has profound implications on the structure of the CDW and its transport properties. In particular, we show how the dynamical generation of dislocations can make the system *more disordered* above the depinning threshold. This result is in agreement with recent x-ray scattering experiments by Ringland *et al.* [1] who observed an increasing correlation length upon letting the CDW relax from the sliding state to the pinned state. This behavior, generic in our model, has not been seen in any of the previously studied theoretical models [19–21]. Furthermore, our results suggest that upon further increasing the drive, the system becomes more ordered. This is in accord with very recent experimental results by Ringland *et al.* [3]. In particular, we predict that the correlation length should increase exponentially. These results are consistent with the picture of Balents and Fisher [12] of a dynamical phase transition into a temporally periodic “moving solid” phase. Finally, we show that the behavior of the dislocation density can be hysteretic upon increasing and decreasing the drive. Indeed, we find that the hysteresis is associated with the activated formation of channels of dislocations. Based on these results we argue that the current in the model should display “switching” (i.e., hysteresis). This is in qualitative agreement with recent transport experiments by Lemay *et al.* [2].

We propose a phenomenological equation of motion, related to the Swift-Hohenberg equation [22], which permits periodic solutions to occur only in the  $x$  direction,

$$\frac{\partial \psi}{\partial t} + E \frac{\partial \psi}{\partial x} = \left[ \epsilon - \left( q_c^2 + \frac{\partial^2}{\partial x^2} \right)^2 + 4 q_c^2 \frac{\partial^2}{\partial y^2} \right] \psi - \psi^3 + \sum_i V_{imp}^i, \quad (1)$$

where  $\psi = \psi(\vec{x}, t)$  denotes the local condensate density, and  $\epsilon \equiv |T - T_p|/T_p$ , with  $T_p$  denoting the critical temperature of the Peierls transition.  $E$  denotes the external drive, and  $V_{imp}^i$  is the localized impurity pinning.  $q_c$  stands for the wavenumber of the periodic modulation

which is set to unity hereafter. Impurities are characterized by a concentration  $c$  and quenched Gaussian correlations  $\langle V_{imp}^i \rangle = 0$  and  $\langle V_{imp}^i V_{imp}^j \rangle = 2V_0 \delta_{ij}$ . The use of both impurity strength  $V_0$  and impurity concentration  $c$  to describe impurities provides a convenient way to tune between weak and strong pinning regimes, as described below. We note that the dynamics of  $\psi$ , in the absence of external drive, follow from the Lyapunov functional:

$$F = \int d\vec{x} \left\{ -\psi \left[ \epsilon - \left( q_c^2 + \frac{\partial^2}{\partial x^2} \right)^2 + 4q_c^2 \frac{\partial^2}{\partial y^2} \right] \frac{\psi}{2} + \psi^4/4 + \sum_i \psi V_{imp}^i \right\}. \quad (2)$$

That is,  $\partial\psi/\partial t = -\delta F/\delta\psi$ . It is straightforward to include the effects of thermal noise [23].

This equation naturally produces periodic structures, permitting the study of local fluctuations in the wavelength, as well as order and defects, as described by the phase and amplitude variations of the charge-density wave. In particular, a second-order derivative is sufficient in the  $y$ -direction since no periodic ordering occurs in that direction, while both second and fourth-order derivatives are necessary in the  $x$ -direction to produce a periodic pattern, and to suppress spatial gradients on very small length scales. Higher-order derivatives in the  $x$  or  $y$  directions may alter the local structure of the defects, but will not qualitatively change the long-range interaction between defects. In the limit of small  $\epsilon$ , it is equivalent to the standard Ginzburg-Landau approach [4,14–16]. The equivalence can be shown via a multiple-scales expansion [23] using the slow variables  $\epsilon t$ ,  $\epsilon^{1/2}x$ , and  $\epsilon^{1/2}y$ , and the ansatz,  $\psi = \epsilon^{1/2}\psi_0 + \epsilon\psi_1 + \epsilon^{3/2}\psi_2 + \dots$ . To leading nontrivial order, we obtain the equation of motion for the complex amplitude  $A$  for the most unstable mode  $\partial A/\partial t = 4(\partial^2/\partial x^2 + \partial^2/\partial y^2)A + A - 3|A|^2 A$ , which is the time-dependent Ginzburg-Landau equation of motion for a complex order parameter, which includes both phase and amplitude fluctuations. The effects of driving force and pinning potential can be straightforwardly included. This, together with an explicit mapping of our approach to that of others, will be given in a future paper [23]. The advantage of our approach is the natural interplay between local variations in wavelength during the dynamical process, which is difficult to isolate in the Ginzburg-Landau equation. Away from threshold,  $\epsilon \sim 1$ , other unstable modes can become important. We expect that, since our equation captures the correct symmetries and essential physics of the driven charge density waves, that it will remain a valid description for large  $\epsilon$ . Indeed,  $q_c$  is only weakly dependent on  $\epsilon$  [24]. Also, our numerical results and tests for varying driving forces and  $\epsilon$  show no qualitative dependence on the size of  $\epsilon$ .

The nature of CDW pinning is determined by comparing the energy gain the wave experiences by adjusting to the local impurities, to the increased elastic energy due that adjustment [25]. The former energy is  $V_0 c \epsilon^{1/2}$ ,

where  $\epsilon^{1/2}$  gives the amplitude of the CDW. The latter is  $\epsilon c \ell^{-2}$ , where  $\epsilon$  gives the elastic force constant, and  $\ell \sim c^{-1/d}$  is the distance between impurities in  $d$  dimensions. In two dimensions, the ratio of these gives a dimensionless parameter  $\kappa = V_0/(c\epsilon^{1/2})$ . Strong pinning corresponds to large  $\kappa$ , weak pinning to small  $\kappa$ . Herein we conveniently tune between regimes by varying  $c$ , so that strong pinning corresponds to small  $c$ .

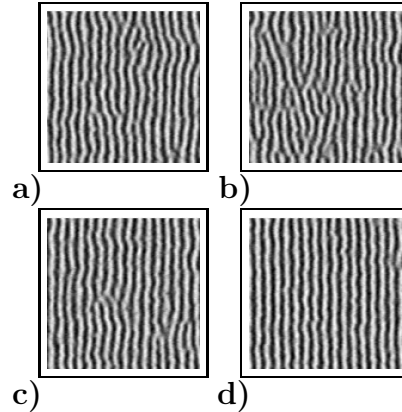


FIG. 1. (a)-(d): Typical configurations. In (a), the external drive  $E = 0$ ,  $V_0 = 0.4$  and  $c = 0.8$ . In (b),  $E = 0.05$ . In (c),  $E = 0.1$ . In (d),  $E = 0.2$ . Only one quarter of the original system size is shown for clarity.

We studied the discretized version of Eq. (1) on a  $d = 2$  square lattice of size  $L = 256$ , where the discretized elements of time and space were  $dt = 0.05$  and  $dx = 0.78$ , respectively. Gradients were evaluated using standard finite differencing. We verified that making  $dt$  and  $dx$  smaller did not change our results. The control parameter,  $\epsilon$ , was varied between 0.1 and 1.2, the pinning strength  $V_0 = 0.1 - 1.5$ , the concentration of pinning sites  $c = 0 - 1$ , and the driving force  $E = 0 - 0.2$ . Results involve averages over at least 10 independent representations of the disorder. Typical configurations of the system are shown in Fig. 1 with  $c = 0.8$  and  $V_0 = 0.4$ . In the relaxed state ( $E = 0$ ), Fig. 1a, some defects are visible. As the driving force is increased past the depinning transition (Fig. 1b with  $E = 0.05$ ) the number of defects  $n_D$  increases [26]. However, for a still larger driving force, defects begin to disappear (Fig. 1c with  $E = 0.1$ ) and, eventually, the system becomes more ordered (Fig. 1d where  $E = 0.2$ ).

We quantify this observation by examining the spherically averaged structure factor  $S(q)$ , defined by  $S(q) = \langle |\hat{\psi}(\vec{q}')|^2 \rangle_{|\vec{q}'|=q}$ , where  $\hat{\psi}$  denotes the Fourier transform of  $\psi$  and  $\langle \dots \rangle_{|\vec{q}'|=q}$  denotes an average over all configurations and Fourier modes with  $|\vec{q}'| = q$ . A typical structure factor is shown in Fig. 2. for a relaxed state  $E = 0$ , and for increasing driving force in the sliding state where  $E > E_c$  ( $E = 0.025$  and  $0.05$ ). As the drive is turned off, the peak of the structure factor increases and, cor-

respondingly, the half width at half maximum decreases. This implies that the correlation length increases upon switching off the drive, in qualitative agreement with recent dynamical x-ray scattering experiments by Ringland *et al.* [1]. Furthermore, upon monotonically increasing the drive we observe a sharpening of the peak, due to decreasing  $n_D$ . This surprising nonmonotonic behavior is in good qualitative accord with recent x-ray scattering experiments by Ringland *et al.* [1,3].

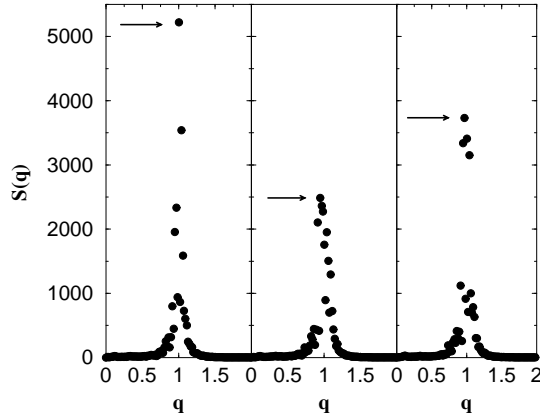


FIG. 2. Structure factor  $S(q)$  for, from left to right,  $E = 0$ ,  $E = 0.075$  and  $E = 0.09$ .  $V_0 = 0.5$  and  $c = 0.8$ .

To further quantify this nonmonotonic dependence, we estimated numerically the number of dislocations  $n_D$  in the system in the following manner. First we determined the number of areas  $n_A$  in the system where the local *transverse* gradient  $|\nabla_y \psi| \geq 0.35$ . We have checked that  $n_A = A \cdot n_D + B$ , where  $A \approx 10$  is the contribution from an isolated defect, and  $B$  is a measure of the roughness of the CDW in the absence of defects, which is dependent on  $c$ . In Fig. 3 we show the number of dislocations  $n_D$  for  $c = 0.4$ , corresponding to the strong pinning regime; the weak pinning result ( $c = 0.8$ ) is shown in the inset. As Fig. 1 indicated, there is an initial increase in  $n_D$ , up to a maximum appearing close to the depinning transition, followed by a subsequent decay for  $E > E_c$ .

The behavior of  $n_D$  and the structure factor can be understood using a simple argument. In the absence of thermal fluctuations, the generation of dislocations must depend on the number density of pinned sites  $n_p$  and on the local strain rate. In addition, annihilation of dislocations depends on the mobility  $D$  and  $n_D$ . In mean-field theory, the rates for generation and annihilation of defects are given by  $R_G \sim n_p \cdot v$  and  $R_A \sim D \cdot n_D$ . The velocity  $v$  of the CDW enters into  $R_G$  since the local strain rate is proportional to the local velocity. Using the above expressions, the mean-field steady-state number of dislocations is simply  $n_D \sim n_p \cdot v$ . Scaling arguments imply [23]  $n_D \sim (E - E_c)^{\theta - \nu}$  as  $E \rightarrow E_c$  and  $n_D \sim \exp -E^2$  as  $E \gg E_c$ , where  $\theta$  and  $\nu$  denote the velocity and cor-

relation length exponents, respectively. Indeed, our data is in good qualitative agreement with these arguments, although our data do not permit a detailed test.

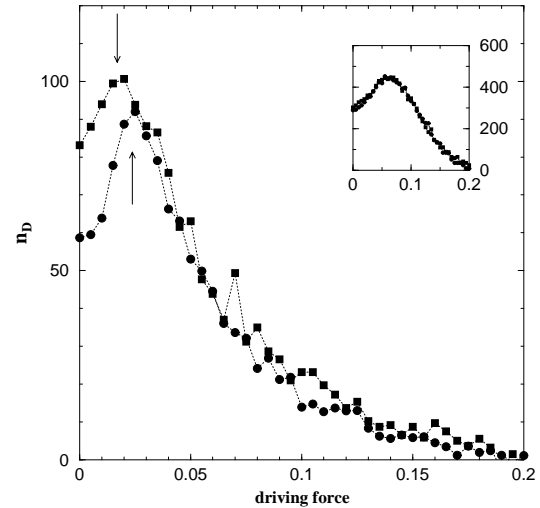


FIG. 3. Number of dislocations  $n_D$  as a function of the driving force  $E$  for strong pinning. Pinning strength  $V_0 = 0.5$  and impurity concentration  $c = 0.4$ . Circles: increasing drive. Squares: decreasing drive. Inset:  $n_D$  for weak pinning ( $c = 0.8$ ).

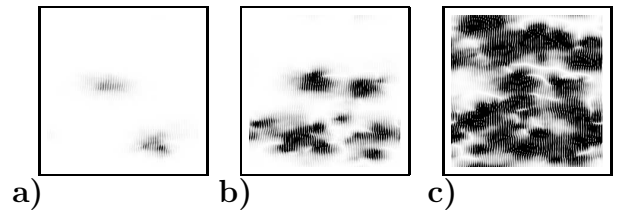


FIG. 4. The behavior of the system near the depinning threshold in the strong pinning regime. Each of the snapshots is a difference between two configurations 500 time steps  $dt$  apart (25 time units since  $dt = 0.05$ ). The black areas indicate where the changes occur, i.e., which areas are moving. The grey scale is the same in all the pictures.  $V_0 = 0.5$ ,  $c = 0.4$ . (a) at  $E = 0.020$ , (b)  $E = 0.025$ , and (c)  $E = 0.030$ .

In the strong pinning regime, additional behavior is evident:  $n_D$  shows significant *hysteresis* as the drive is first increased and then decreased. In the weak pinning limit, no significant hysteresis is seen. The origin of this is evident in Fig. 4. We compare two configurations of the same system at different time steps, around the depinning threshold. The configurations were taken 500 time steps  $dt$  apart (25 time units since  $dt = 0.05$ ), and then they were deducted from each other. The darker areas indicate where the changes are the largest. Below the threshold, in the strong pinning regime, there is little movement in the system. As the driving force is increased to the transition, a conducting channel appears. As the driving

force is increased further, the system depins coherently. In other words, depinning in the strong pinning regime is mediated by activated channels [27].

In contrast, in the weak pinning regime (not shown) domains form cooperatively, even before depinning takes place, and the transition takes place collectively, with insignificant apparent activation. Unfortunately, in our two-dimensional simulations, we cannot determine if the qualitative transition in behavior between weak and strong pinning is sharp, or governed by crossover. The qualitative difference is easy to understand. In the strong-pinning regime, impurities are far apart, so channels, where regions of current flow, “nucleate” between impurities. In the weak pinning regime, where there are more impurities, there is insufficient room for channels to form, and, instead, a cooperative and collective effort of the entire system is required to depin the system. This bistable behavior in the strong pinning regime will manifest itself in the current-voltage characteristics of the sample. This is known as “switching”, and is a generic feature of low-temperature CDWs [2,28–30]. This behavior, which follows naturally from our approach, is in qualitative agreement with recent transport measurements of Lemay *et al.* [2].

In conclusion, we have introduced a novel approach to study the of driven charge-density waves. We have demonstrated that, above the global depinning threshold, phase slips appear and lead to an even more disordered structure for the CDW, as seen experimentally [1]. However, far away from threshold the system becomes more ordered, as observed very recently [3]. These latter results are in agreement with the picture of Balents and Fisher [12]. Finally our model gives rise to a simple and generic mechanism for switching in the strong pinning regime, through the activated appearance of channels, which qualitatively explains recent experimental results [2].

We thank the authors of Refs. [1–3], particularly Joel Brock, for useful discussions and for communicating their work to us prior to publication. We thank Mark Sutton for useful discussions. This work has been supported by the Academy of Finland (MK & MH), the Finnish Cultural Foundation (MK), the Finnish Academy of Science and Letters (MK), Research Corporation grant CC4787 (KRE), the Natural Sciences and Engineering Council of Canada (MG), *le Fonds pour la Formation de Chercheurs et l’Aide à la Recherche du Québec* (MG).

---

[1] K. L. Ringland et al., Phys. Rev. Lett. **82**, 1923 (1999).

[2] S. G. Lemay, R. E. Thorne, Y. Li, and J. D. Brock, Phys. Rev. Lett. (in press, 1999).

- [3] K. L. Ringland et al., Submitted for publication (1999).
- [4] G. Grüner, Rev. Mod. Phys. **60**, 1129 (1988).
- [5] D. S. Fisher, M. P. A. Fisher, and D. A. Huse, Phys. Rev. B **43**, 130 (1991).
- [6] A. E. Koshelev and V. M. Vinokur, Phys. Rev. Lett. **73**, 3580 (1994).
- [7] J. Hu and R. M. Westervelt, Phys. Rev. B **51**, 17279 (1995).
- [8] R. E. Peierls, *Quantum Theory of Solids*, Oxford University Press, New York, 1955.
- [9] S. N. Coppersmith, Phys. Rev. Lett. **65**, 1044 (1990).
- [10] S. N. Coppersmith, Phys. Rev. B **44**, 2887 (1991).
- [11] S. N. Coppersmith and A. J. Millis, Phys. Rev. B **44**, 7799 (1991).
- [12] L. Balents and M. P. A. Fisher, Phys. Rev. Lett. **75**, 4270 (1995).
- [13] C. Tang, K. Wiesenfeld, P. Bak, S. Coppersmith, and P. Littlewood, Phys. Rev. Lett. **58**, 1161 (1987).
- [14] H. Fukuyama, J. Phys. Soc. Japan **41**, 513 (1976).
- [15] H. Fukuyama and P. A. Lee, Phys. Rev. B **17**, 535 (1978).
- [16] P. A. Lee and T. M. Rice, Phys. Rev. B **19**, 3970 (1979).
- [17] S. Ramakrishna, M. P. Maher, V. Ambegaokar, and U. Eckern, Phys. Rev. Lett. **68**, 2066 (1992).
- [18] C. Zeng, P. L. Leath, and D. S. Fisher, Phys. Rev. Lett. **82**, 1935 (1999).
- [19] P. Sibani and P. B. Littlewood, Phys. Rev. Lett. **64**, 1305 (1990).
- [20] A. A. Middleton, Phys. Rev. Lett. **68**, 670 (1992).
- [21] L. W. Chen, L. Balents, M. P. A. Fisher, and M. C. Marchetti, Phys. Rev. B **54**, 12798 (1996).
- [22] J. Swift and P. C. Hohenberg, Phys. Rev. A **15**, 319 (1977).
- [23] M. Karttunen, M. Haataja, K. R. Elder, and M. Grant, In preparation (1999).
- [24] Y. Pomeau and P. Manneville, J. Physique Lett. (Paris) **23**, L (1979).
- [25] G. Grüner, *Density Waves in Solids* (Addison Wesley, Reading Massachusetts, 1994).
- [26] The position of the depinning transition  $E_c$  was determined by measuring where the average current  $I$ , estimated by  $I \propto |v_x|/L^2$  becomes nonzero. The depinning transition is somewhat to the left of the peak in  $n_D$  in Fig. 3. This measure of  $I$  does not distinguish dislocations from periodic waves, and so does not give the current-voltage characteristics for  $E > E_c$ . In a future long paper [23], we will discuss the relationship of  $E_c$  to the threshold field in, for example, the Fukuyama-Lee-Rice model.
- [27] L. Balents, ITP Online Lecture Notes and Review Articles, 1996.
- [28] A. Zettl and G. Grüner, Phys. Rev. B **26**, 2298 (1982).
- [29] R. P. Hall and A. Zettl, Solid State Comm. **50**, 813 (1984).
- [30] R. P. Hall, M. F. Hundley, and A. Zettl, Phys. Rev. B **38**, 13002 (1988).